Available online at www.sciencedirect.com
SCIENCE DIRECT®
Journal of Power Sources 124 (2003) 191–196
JOURNAL OF POWER SOURCES
www.elsevier.com/locate/jpowsour

Rate capability of natural Swedish graphite as anode material in Li-ion batteries

M. Herstedt, L. Fransson, K. Edström*

Department of Materials Chemistry, Ångström Laboratory, Uppsala University, P.O. Box 538, SE-751 21 Uppsala, Sweden

Received 17 December 2002; accepted 20 May 2003

Abstract

Jet-milled natural Swedish graphite has been evaluated as an anode material for Li-ion battery applications, with a focus on rate capability of the material. The material was found to have a superior rate capability compared to other carbon materials with similar particle sizes. It could also intercalate and deintercalate lithium reversibly in an electrolyte based on propylene carbonate:ethylene carbonate (1:1). Jet-milling was found to increase the amount of rhombohedral phase (3R) in the material from 15 to 40%. However, after repeated electrochemical intercalation and deintercalation of lithium, the amount of 3R phase decreases to ∼5%. Neither rate capability nor PC-tolerance can therefore be correlated to the amount of 3R phase.

Keywords: Natural graphite; Jet-milling; Rate capability; Rhombohedral phase

1. Introduction

Graphitic carbon is the most commonly used anode material in today's commercial lithium-ion batteries. However, two main aspects need to be improved to achieve better performance and a higher level of safety: capacity and rate capability. From an economic point of view, natural graphite is the obvious choice as anode material compared to other carbonaceous materials. It also exhibits a high capacity through its high degree of crystallinity and low, flat potential profile versus lithium. Natural graphite contains two phases: predominantly hexagonal (2H), with a small fraction of a rhombohedral (3R) phase. Much work has appeared describing the influence of the 3R phase on the performance of the lithium-ion battery. Shi et al. have reported that there is no apparent difference between the lithium intercalation capacities of the two graphite phases [1], while Huang et al. later correlated an increased intercalation capacity to larger 3R phase content [2]. The latter authors claimed that additional lithium could be intercalated into the phase-boundary regions between the 2H and 3R phases. Another aspect was noted by Guerin et al.; graphite with >30% 3R phase is able to intercalate lithium ions in propylene carbonate (PC)-based electrolytes, contrary to the behaviour of most graphite materials. This tentatively attributed this interesting observation to the presence of defects, which create a favourable surface morphology to prevent the co-intercalation of PC [3]. PC is a good electrolyte component for low-temperature battery applications due to its low melting point (−54.5 °C) and relatively high conductivity. Since 3R phase content would seem advantageous, it is therefore interesting to investigate alternative ways to promote its formation. Previously, it has been shown that mechanical grinding and ultrasonic treatment can increase the amount of 3R phase [3].

Ball-milling is an effective method for reducing particle size. It also induces defects and the breaking up of crystalline structures to produce a more amorphous graphite structure. There are many reports of the influence of ball-milling of graphite on its atomic structure and lithium intercalation properties [4–6]. Jet-milling has been described in recent patents for obtaining spherical or rounded graphite particles favourable for high performance anodes in Li-ion batteries [7,8]. Wang et al. have shown that jet-milling reduces the particle size in a less destructive way than ball-milling, and results in an increased reversible capacity [9]. However, the influence of jet-milling on the rate capability and amount of 3R phase was not addressed.

We present here an investigation of the effect of jet-milling on rate capability, i.e. the ability to intercalate and deintercalate lithium ions under high current density. Results from a new Swedish natural graphite, both raw and jet-milled, are

* Corresponding author. Tel.: +46-18-4713713; fax: +46-18-513548.
E-mail address: kristina.edstrom@mkem.uu.se (K. Edström).

0378-7753/$ – see front matter © 2003 Elsevier B.V. All rights reserved.
doi:10.1016/S0378-7753(03)00603-7

presented and compared to results from commercially available graphites. The effect of jet-milling on the amount of 3R phase was also investigated. More importantly, the amount of 3R phase after repeated intercalation and deintercalation of lithium ions was also studied by ex situ XRD.

2. Experimental

2.1. Powder characterisation

Natural graphite, Woxna fine grade (99.8%), was used *as received* and after jet-milling. The jet-milling was performed using an Alpine jet mill 100 AFG at a rate of 22,000 rpm (∼367 Hz). An α-Al_2O_3 (corundum) wheel was used with three nozzles with a diameter of 1.9 mm. The powder particle size distribution was analysed using a Malvern Mastersizer [10] and the surface areas were determined by gas adsorption in a standard BET measurement. SEM pictures were obtained using a Field Emission Scanning Electron Microscope, LEO 1550. The impurities in the graphite were identified with a Link Energy-Dispersive Spectrometer (EDS) on a JEOL JSM 840 SEM.

The XRD measurements were performed on a Stoe and Cie GmbH STADI powder diffractometer equipped with a Ge(1 1 1) monochromatized Cu $K_{\alpha 1}$ radiation source. Diffractograms were recorded in transmission mode between 20 and 90° in 2θ with a position-sensitive detector (PSD). A 0.7 mm diameter glass capillary was used as sample holder to minimise preferred orientation effects. The average spacing between the graphene layers, d(0 0 2), was calculated from the position of the 0 0 2 reflection. The crystallinity parameters L_c(0 0 2) and L_a(1 0 0) were calculated using Scherrer's modified formula for carbon [11]; the amount of 3R phase was calculated using the Rietveld method [12]. The effect of repeated electrochemical cycling on the amount of 3R phase was investigated ex situ by XRD, using a PSD centred at 45° in 2θ, for electrode material extracted from a cell cycled 25 times.

2.2. Electrochemical characterisation

Electrodes were manufactured with 80 wt.% active material, 10 wt.% carbon black (Shewinigan Black) and 10 wt.% ethylene propylene diene terpolymer (EPDM) binder. The active materials were Swedish natural graphite (raw and jet-milled), Osaka Gas carbon microbeads (SGBII) or Brazilian natural graphite (MP). All electrodes were circular discs with area 3.14 cm^2 and ca. 4 mg active material. The electrochemical performance was evaluated in half-cells (graphite versus lithium), with electrolyte either 1 M $LiPF_6$ in EC:DMC (2:1) or 1 M $LiPF_6$ in EC:PC (1:1) by volume, assembled in the "coffee-bag" configuration [13]. The half-cells were cycled at constant current rate C/8 for 25 cycles using a Digatron BTS-600. The cells were also rate-tested galvanostatically and compared to reference carbons with similar particle size. The reference materials selected were natural graphite from Brazil (MP) and microbeads (SGBII). The rate capability test was performed using the following protocol (current densities are given within parentheses): the cells were cycled at C/8 (43 mA g^{-1}) for eight cycles, at C/4 (93 mA g^{-1}) and at C/2.5 (149 mA g^{-1}) for four cycles, and back to C/8 for the last four cycles.

3. Results and discussion

3.1. Powder characterisation

The SEM micrographs for raw and jet-milled natural Swedish graphite (Fig. 1) show that the particles retain their flake-like shape during jet-milling, although the particle size is reduced. EDS analysis identified the impurities (0.2% in total) to be traces of Al, Si, K, S and Fe. Jet-milling exposed more impurities, probably located in the grain boundaries, which had not been removed during chemical purification and, because of the small penetration depth of EDS (1.5 μm), could not be detected in unmilled samples.

The X-ray diffraction patterns of raw and jet-milled graphite (Fig. 2) show that the graphite retains its well-ordered structure after jet-milling, albeit the background is

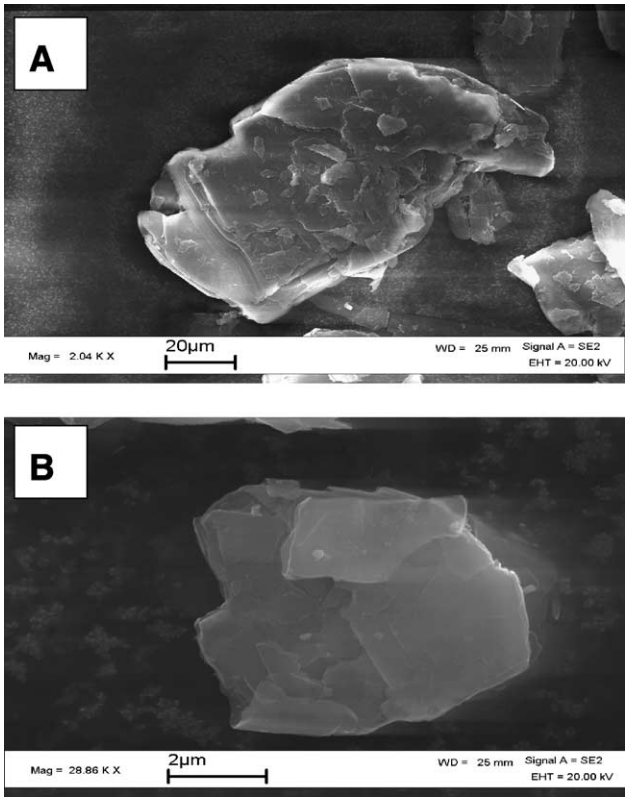

Fig. 1. SEM micrographs of particles of (A) raw and (B) jet-milled natural Swedish graphite.

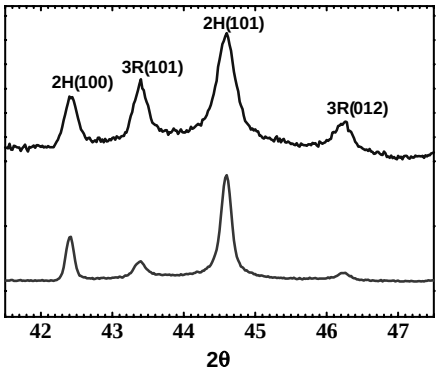

Fig. 2. X-ray diffraction pattern of raw (lower trace) and jet-milled (upper trace) graphite.

ca. three times higher for the jet-milled samples because of larger contributions from amorphous material. A clear difference is seen in the diffraction patterns between 42 and 48° in 2θ. The 3R peaks at 43.36° (1 0 1) and 46.22° (0 1 2) in 2θ are clearly more discernible for the jet-milled sample. The amount of 3R phase was calculated using the Rietveld method [12] and found to increase from 15 to 40% after jet-milling. The structural and surface-area parameters for raw and jet-milled graphite are summarised in Table 1. The size of the graphite crystallites was found to show a decrease in L_c(0 0 2), whereas L_a(1 0 0) remained more or less unchanged after jet-milling. Jet-milling also increases the *d*-values slightly, as expected when more 3R phase is formed [14]. However, it should be noted that the change in *d*-spacing is not as severe as for ball-milling [15]. The particle size, measured as the d_{50} parameter [10], decreases from ~80 to 8 μm upon jet-milling. At the same time, the surface area increases from 3.8 to 10.9 $m^2\,g^{-1}$. Micro-Raman spectra (not given) showed no changes in surface morphology induced by jet-milling.

3.2. Electrochemical characterisation

A summary of the cycling results is presented in Table 2. Jet-milling clearly has a positive effect on the reversible capacity. The irreversible capacity, however, is also higher, as is commonly found when the reversible capacity or the surface area increases [16,17]. The higher capacity for the jet-milled material is assumed to be mainly a result of the reduced particle size. To verify this, the deintercalation capacity of the raw graphite was investigated at a 10 times slower current density (*C*/80), since the particles in the raw sample are ~10 times larger than in the jet-milled case. Not surprisingly, this resulted in a deintercalation capacity of ~350 mA h g^{-1} similar to that for jet-milled graphite. It is worth noting that the deintercalation capacity has decreased after 25 cycles (compared to the first cycle) for jet-milled graphite, whereas raw graphite shows the opposite behaviour (Table 2). The former result is likely to be due to impurities, which are exposed in the jet-milling process. The latter behaviour could be due to electrochemical grinding of the particles during cycling, leading to better utilisation of the electrode material. Jet-milling, like ultrasonification [3], also makes the graphite more PC-tolerant. It can cycle reversibly in a PC:EC (1:1) electrolyte, whereas the raw material is unable to intercalate lithium ions in the same electrolyte (Table 2). Our results are in agreement with earlier work [2,3], which showed that graphites with enhanced amounts (>30%) of the 3R phase are PC-tolerant and exhibit an improved reversible capacity. However, we show below that it is not necessarily the 3R phase itself that is directly responsible for the improved performance.

3.3. Rate capability tests

Factors affecting the rate capability include graphite particle size (determining lithium diffusion within the

Table 1
Structural and surface properties of raw and jet-milled natural Woxna graphite

Sample	*d*(0 0 2) (Å)	L_c(0 0 2)[a] (Å)	L_a(1 0 0)[a] (Å)	d_{50} (μm)	BET ($m^2\,g^{-1}$)	Amount of 3R-phase[b] (%)
Jet-milled	3.3546 (4)	475	>1000	8.0	10.9	40
Raw	3.3524 (3)	581	>1000	~80	3.8	15

[a] Calculated using the modified Scherrer formula [11].
[b] Calculated using Rietveld refinement [12].

Table 2
Summary of electrochemical performance for different graphites cycled in an electrolyte containing 1 M $LiPF_6$ and the solvents stated

Sample	Intercalation capacity first cycle (mA h g^{-1})	Deintercalation capacity first cycle (mA h g^{-1})	Irreversible capacity first cycle (%)	Intercalation capacity 25th cycle (mA h g^{-1})	Columbic efficiency 25th cycle (%)	First cycle irreversible capacity/surface area (mA h m^{-2})
Raw EC:DMC	397	330	17	339	99.8	17.8
Jet-milled EC:DMC	493	371	25	365	99.9	11.2
Raw PC:EC	>800[a]	0	100	–	–	–
Jet-milled PC:EC	577	364	37	345	95.8	19.5
MP EC:DMC	419	345	17	352	100	9.1
SGBII EC:DMC	353	298	15	293	99.8	13.8

[a] The experiment was interrupted after 800 mAh at a potential approx. 0.8 V.

particle), electronic conductivity and transport rate for lithium ions across the SEI layer. Poor rate capability will lead to severely reduced capacity at higher current densities. Since the rate capability depends partly on the particle size [18], the jet-milled graphite is expected to show a better rate capability than the raw material. This is clearly confirmed in Fig. 3a, where the reversible capacities at different current densities are shown for jet-milled and raw graphite. The decrease in capacity at higher current densities is smaller for the jet-milled graphite than for the raw material.

More importantly, the rate capability for the jet-milled graphite is superior to that of other carbons of similar particle size, as seen in Fig. 3b (for a description of the reference materials, see Experimental and Table 3). The jet-milled graphite maintains a stable capacity at higher current densities, while the reference materials show a rapidly declining capacity as the current density is increased. The enhanced rate capability for jet-milled graphite cannot therefore be attributed *solely* to smaller particle size.

Table 3
The properties of microbeads (SGBII) and natural Brazilian graphite (MP)

	SGB-II	MP
Purity (%)	99.65	99.93
Density ($g\,cm^{-3}$)	0.40	0.20
BET ($m^2\,g^{-1}$)	4.0	8.1
Particle size d_{50} (μm)	7.0	9.6

Surface properties also influence the rate capability. It is therefore surprising that the reference materials, with much

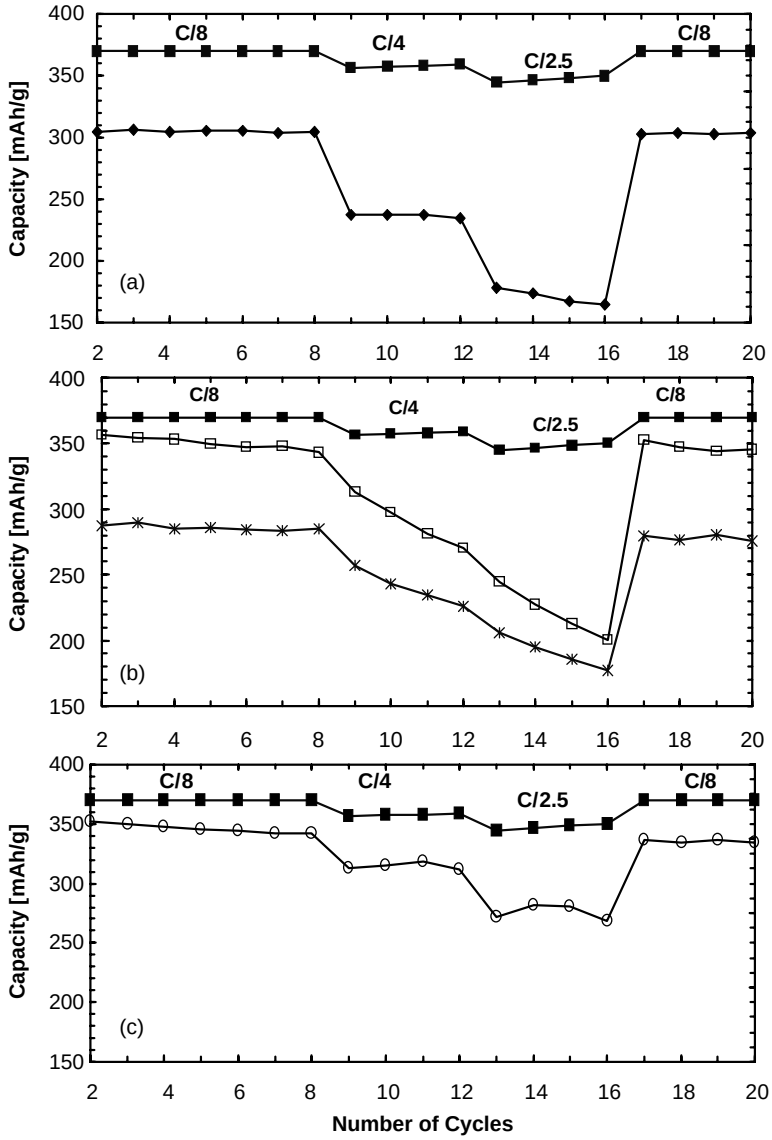

Fig. 3. The deintercalation capacity at different current densities for: (a) raw (◆) and jet-milled (■) graphite; (b) MP (□), SGBII (✳) and jet-milled (■) graphites. The electrolyte used in (a) and (b) was 1 M $LiPF_6$ EC:DMC (2:1); and (c) jet-milled graphite in 1 M $LiPF_6$ EC:DMC (2:1) (■) and 1 M $LiPF_6$ PC:EC (1:1) (○).

lower irreversible capacities than the jet-milled graphite, show an inferior rate capability. To help elucidate this, we have calculated the area-specific irreversible capacities for each material, and found them to vary less than the irreversible capacity (Table 2). This suggests that bulk properties dominate the rate capability behaviour of the materials studied here.

The rate capability for jet-milled graphite in two different electrolytes is shown in Fig. 3c. The decrease in capacity at higher current densities is slightly greater for the PC-based electrolyte, which would suggest the formation of an SEI layer with slower lithium-ion transport properties. The area-specific irreversible capacity is substantially higher for the PC-electrolyte (Table 2). This indicates an SEI layer of different composition and/or thickness.

These findings combined to indicate that it is the bulk structure of the jet-milled graphite that mainly determines the rate capability. From Table 1, it is clear that the main difference induced by jet-milling is the amount of 3R phase. It is therefore of great interest to investigate the 3R phase further and how its relative amount is affected by electrochemical cycling.

3.4. The effect of cell cycling on the amount of 3R phase

It is well known that, when lithium ions intercalate into the hexagonally packed graphene sheets of graphite, the ABA... stacking changes to an AAA... stacking in LiC_6, and that this structure change is reversible. Lithium-ion intercalation in the 3R phase also leads to an AAA... stacking of the planes [1], but it is not clear whether the graphene sheets regain their ABCA... stacking as the lithium ions are extracted; the enthalpy difference between the 2H and 3R phases is only $0.6\,kJ\,mol^{-1}$ [14]. XRD patterns from fresh and electrochemically cycled jet-milled graphite are shown in Fig. 4. The fresh material exhibits two clearly distinguishable peaks from the 3R phase (1 0 1 and 0 1 2 at 43.36 and 46.22° in 2θ, respectively). These peaks are diminished for the electrochemically intercalated and deintercalated material, showing that the amount of 3R phase is not constant. Instead, a majority of the 3R phase transforms to the 2H structure after lithium extraction. This shows that the improved rate capability *cannot* be correlated to the amount of 3R phase. Previous studies have shown that 3R-content >30% gives a PC-tolerant graphite. This behaviour has tentatively been attributed to surface defects [3]. Surface defects can be have been created in two ways: (i) particles collisions and/or (ii) graphene planes changing from ABA... to ABCA... stacking. In the first case, the increase in 3R phase may be regarded as a measure of the defect concentration; in the second case, the increase is responsible for the defect concentration. Therefore, the amount of 3R phase may not be the essential parameter, but rather the magnitude of the *increase* in 3R phase present. The jet-milled graphite can have a surface morphology resembling that of graphite coated with a layer of amorphous carbon; both found to cycle reversibly in a PC-based electrolyte [19].

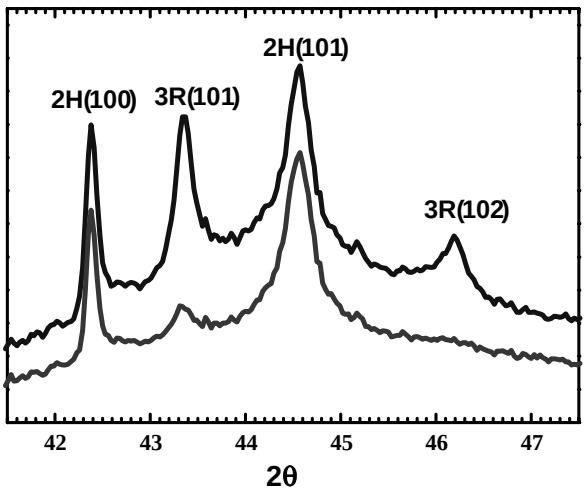

Fig. 4. Part of the XRD pattern for uncycled (upper trace) and cycled jet-milled graphite (lower trace). The graphite was cycled 25 times in 1 M $LiPF_6$ EC:DMC (2:1).

4. Conclusions

Jet-milled natural Swedish graphite is found to have a rate capability superior to that of other carbons of similar particle size. This can be attributed mainly to its favourable bulk structure, which is retained after jet-milling. Furthermore, jet-milling is found to increase the amount of 3R phase from 15 to 40%. Like other graphites with 3R phase content above 30%, the jet-milled graphite can intercalate and deintercalate lithium reversibly in an electrolyte consisting of PC:EC (1:1). Jet-milled graphite can thus be considered as PC-tolerant. However, it would appear that the *increase* in 3R phase content during jet-milling is the critical factor and not the amount of 3R phase, since this is seen to disappear on electrochemical cycling.

Acknowledgements

This work has been supported by The Foundation for Environmental Strategic Research (MISTRA), The Swedish Technical Science Research Council (TFR), The Swedish Science Council (VR) and The Nordic Energy Research Programme (NERP). The authors would also like to acknowledge Tricorona Mineral AB, Sweden for supplying the Woxna graphite and assisting with the jet-milling and BET measurements. We also thank Dr. Kajsa L. Björklund for SEM making the micrographs, Dr. Michael Tucker for proof reading and Professors Roland Tellgren and Josh Thomas (all of the Department of Material Chemistry at Uppsala University) for many fruitful discussions.

References

[1] H. Shi, J. Baker, M. Saidi, R. Koksbang, J. Electrochem. Soc. 143 (1996) 3466.
[2] H. Huang, W. Liu, X. Huang, L. Chen, E.M. Kelder, J. Schoonman, Solid State Ionics 110 (1998) 173.
[3] K. Guerin, A. Fevrier-Bouvier, S. Flandrois, M. Couzi, B. Simon, P. Biensan, J. Electrochem. Soc. 146 (1999) 3660.
[4] F. Disma, L. Aymard, L. Dupont, J.-M. Tarascon, J. Electrochem. Soc. 143 (1996) 3959.
[5] F. Salver-Disma, R. Fahri, C. Guery, J.-M. Tarascon, Mol. Cryst. Liq. Cryst. Sci. Technol. A310 (1998) 219.
[6] C. Natarajan, H. Fujimoto, A. Mabuchi, K. Tokumitsu, T. Kasuh, J. Power Sources 92 (2001) 187.
[7] A. Guerfi, F. Brocho, K. Kinoshita, K. Zaghib, Patent WO2002034670 (2002).
[8] S. Kubota, J. Yasumaru, S. Asada, Japanese Patent JP2002179419 (2002).
[9] H. Wang, T. Ikeda, K. Fukuda, M. Yoshio, J. Power Sources 83 (1999) 141.
[10] A. Rawle, The Basic Principles of Particle Size Analysis, Malvern Instruments Ltd., Worcs., UK, 2001.
[11] K. Kinoshita, Carbon: Electrochemical and Physicochemical Properties, Wiley, New York, 1988, p. 33.
[12] J. Rodriguez-Carvajal, in: Proceedings of the Abstracts of the Satellite Meeting on Powder Diffraction of the XVth Congress of the IUCr, Toulouse, France, 1990, p. 127.
[13] T. Gustafsson, J.O. Thomas, R. Koksbang, G.C. Farrington, Electrochim. Acta 37 (1992) 1639.
[14] T.C.W. Mak, G.-D. Zhou, Crystallography in Modern Chemistry, Wiley/Interscience, New York, 1992, p. 44.
[15] F. Salver-Disma, C. Lenain, B. Beudoin, L. Aymard, J.-M. Tarascon, Solid State Ionics 98 (1997) 145.
[16] R. Yazami, J. Power Sources 97–98 (2001) 33.
[17] M. Winter, P. Novak, A. Monnier, J. Electrochem. Soc. 145 (1998) 428.
[18] K. Zaghib, F. Brochu, A. Guerfi, K. Kinoshita, J. Power Sources 103 (2001) 140.
[19] M. Yoshio, H. Wang, K. Fukunda, Y. Hara, Y. Adachi, J. Electrochem. Soc. 147 (2000) 1245.